Geomorphology 414 (2022) 108397

Contents lists available at ScienceDirect

Geomorphology

journal homepage: www.journals.elsevier.com/geomorphology

Invited review

A global review of subaqueous spreading and its morphological and sedimentological characteristics: A database for highlighting the current state of the art

Monica Giona Bucci [a,*], Aaron Micallef [a,b], Morelia Urlaub [b], Joshu Mountjoy [c], Rachel Barrett [d]

[a] University of Malta, Marine Geology and Seafloor Surveying, Faculty of Sciences, Department of Geosciences, Malta
[b] GEOMAR Helmoltz Centre for Ocean Research Kiel, Germany
[c] National Institute of Water & Atmospheric Research Ltd (NIWA), New Zealand
[d] Marine Geophysics and Hydroacoustics, Christian- Albrechts-Universität zu Kiel, Germany

ARTICLE INFO

Keywords:
Subaqueous spreading
Clay softening
Liquefaction
Spreading morphology
Database
Earthquake

ABSTRACT

Subaqueous spreading, a type of extensional mass transport that is characterized by a ridge and trough morphology, has been documented globally but is poorly understood. Subaqueous spreading is observed on gently inclined surfaces (typically <3°) when sediment bodies experience a sudden reduction of shear strength along their basal plane during clay softening or liquefaction of sands or silty sand sediment. Historically, spreading has been associated with very large landslides, but many unknown aspects of these mass movements have yet to be clarified. Does spreading influences the large catastrophic failure? What are the sedimentological and morphological aspects that contribute in initiating this process? These are some of the research questions that spurred the present work. Here, we introduce a database that incorporates information from thirty-two case studies, and use this to provide key insights into the sedimentary and morphological aspects of subaqueous spreading that will assist in the identification of spreading elsewhere. We find that subaqueous spreading is most common along passive glacial margins, but is also observed along active margins. The occurrence of contourites interlayered with glaciogenic deposits is, in most cases, associated with landslides (or landslide complexes) with spreading morphology. The database shows that seismic loading is commonly suggested to be the dominant trigger mechanism, although more geotechnical observations and modelling analysis would be needed to support this conclusion. We compare subaqueous spreading with terrestrial spreading, in particular to earthquake-related lateral spreading and clay landslides. We find that subaqueous spreading shares the same driving processes and potentially also some of the trigger mechanisms that are associated with the terrestrial spreading cases. Future work will be required to address the association between spreading and its occurrence on some of the largest landslides on Earth, its development mechanism, and its potential hazard implications.

1. Introduction

Subaqueous landslides occur across all types of continental margins, in lakes and in fjords, and involve the downslope movement of sediment or rock bodies. Some of the largest landslides ever observed on Earth are subaqueous landslides of at least two orders of magnitude larger than terrestrial landslides (Collot et al., 2001; Vanneste et al., 2006; Urgeles and Camerlenghi, 2013). The Storegga Slide, for example, located off the Norwegian coast is considered amongst the largest landslide on Earth (Masson et al., 2006), with a volume of 2400 to 3200 km^3, an area of ~95,000 km^2, and a run out distance of nearly 400 km (Haflidason et al., 2004; Bryn et al., 2005). The environmental and economic significance of subaqueous landslides has been investigated over the last twenty years, with a particular focus on the risk to nearshore and offshore infrastructures, and tsunami hazard modelling investigations (Talling et al., 2014; Clare et al., 2017). The advent of higher resolution geophysical techniques would allow the investigation of seafloors and the bottom of lakes with the same resolution that is possible on land (Savini et al., 2022), for example by using airborne geophysics, and thus improve the mitigation strategies of subaqueous landslides especially for vulnerable coastal communities.

Spreading is defined as a ground failure that occurs on gently

* Corresponding author.
E-mail address: monica.giona-bucci@um.edu.mt (M. Giona Bucci).

https://doi.org/10.1016/j.geomorph.2022.108397
Received 23 May 2022; Received in revised form 1 August 2022; Accepted 1 August 2022
Available online 5 August 2022

inclined slopes by extensional displacement along a gliding plane (Youd, 1978). Previous authors have distinguished between two main types of spreading based on the material involved: rock spreading (Conti and Tosatti, 1993; Magri et al., 2008; Pasuto and Soldati, 2013; Pasuto et al., 2022) and soil spreading (Pasuto and Soldati, 2013; Pasuto et al., 2022). Thorough analysis of the development of rock spreading can be found in other venues (Pasuto and Soldati, 2013; Pasuto et al., 2022). In particular, recent works have also given emphasis to cases where rock spreading occurred onshore, along the coastline, but developed offshore (Soldati et al., 2018; Prampolini et al., 2019).

Soil spreading is a mass transport process that involves the extensional movement of a sub-horizontal body made of coherent and cohesive sediment (clay or silty clay) over a gliding plane that has experienced a loss of shear strength. This can be due to softening, in the case of clay, or liquefaction, in the case of fine granular material such as silt, silty sands or very fine sand (Hungr et al., 2014).

Subaqueous spreading was first investigated in detail within the Storegga, Traenadjupet and Nyk Slides offshore Norway (Kvalstad et al., 2005; Micallef et al., 2007 and references therein). Up until then, subaqueous spreading had been documented at other large landslides offshore Canada (Piper et al., 1999; Piper, 2005) and the Canary Islands (Krastel et al., 2001), but had not been defined as such or included in offshore mass movement classifications (Mulder and Cochonat, 1996). Spreading is a type of subaqueous mass movement that has been recognized as being hazardous to seafloor and coastal infrastructure (Kvalstad et al., 2005; Baeten et al., 2013; Mountjoy et al., 2018), but also of being a potential for tsunami hazard, in the case of spreading in lakes and fluvial systems (Liu et al., 2021). Micallef et al. (2007) reported that up to 25 % of the Storegga Slide is characterized by ridges and troughs, which are aligned parallel or sub-parallel to the headwall. These ridges and troughs tend to be more closely spaced and more continuous proximal to the headwall of the landslide, but can also occur in the downslope portion of the landslide body, where they tend to result from compression (Schnellmann et al., 2005). In some cases, spreading ridges may present acoustically transparent facies that suggest plastic deformation (Baeten et al., 2013). In contrast, spreading ridges and troughs in other case studies are more distinguishable, such as offshore NW Australia, where Wu et al. (2021) found ridges with no or minimal deformation, suggesting that the blocks had moved over a limited distance. In that study, pore water venting structures (pipes) were observed at the bottom of the troughs, and were suggested to have likely contributed to the gradual widening of the space between the topographic highs (ridges) to accommodate the venting of the over-pressured layers located underneath (Wu et al., 2021).

Because of a general lack of geophysical data and sediment samples, numerical modelling studies have been used to better understand subaqueous spreading (Kvalstad et al., 2005; Puzrin et al., 2015; Dey et al., 2016). These models consider a fully weakened layer (sensu Locat et al., 2014) that fails along a weaker surface (shear band propagation, SBP, Puzrin and Germanovich, 2005; Quinn et al., 2011, 2012; Dey et al., 2015). Essential to the numerical models for spreading is the occurrence of a clay, or silty clay, unit in the stratigraphic profile, which undergoes a strain softening process that allows the propagation of the shear band throughout the sediment body. Toe erosion is one of the major preconditioning mechanisms tested (Dey et al., 2015; Wang, 2020; Wang et al., 2020; Wu et al., 2021). However, those studies showed that toe erosion is not, by itself, sufficient to generate horst and graben morphology. Rather, the geological properties of the spreading sediment: layering, the occurrence of crust (sensu Ishihara, 1985; and then rediscussed in Dey et al., 2016; Perret et al., 2019), and having undrained conditions (i.e. higher pore water pressure), seem to play a more important role (Micallef et al., 2007; Dey et al., 2016; Perret et al., 2019). Some of these simulations have also attempted to explain the link between the occurrence of spreading and the potential for catastrophic failure (Dey et al., 2016). In addition, Dey et al. (2016) is particularly conclusive in linking the development of spreading to the morphology observed both onshore and offshore. The numerical simulations proposed by Dey et al. (2016) showed that horsts and grabens (or ridges and troughs, as defined in the subaqueous realm) occur mainly in the upslope area near the headwall where the extensional domain of the slide is located (sensu Bull et al., 2009). The gravitational downward displacement of the failed sediment blocks reduces the grabens' height at a faster rate than that of the horsts, so that compressional ridges form towards the near end of the slope. When the shear band propagates across a sufficiently long distance, the upper sediment layers will start to fail leading to failure of the entire slope. As a consequence of this, multiple shear surfaces that accommodate multiple shear bands are observed, and a number of tabular glide blocks might form that displace downward, and follow an independent movement over the basal shear zone (Dey et al., 2016). These conditions have been simulated assuming a shearing unit with clay or silty clay, and yet questions remain unaddressed when considering other litho-stratigraphic units (e.g. sands and silty sands) in subaqueous spreading, which can still fail catastrophically even when the shear band propagation approach cannot be adopted (Field et al., 1982; Mountjoy et al., 2009; Nouguès et al., 2009; Crutchley et al., 2022). Furthermore, the limited understanding of the typical sedimentary architecture, as well as the sedimentological and stratigraphic characteristics of spreading, results in a lack of understanding of its development mechanism(s), potential extent of the failed material, and how spreading is preconditioned by the local sedimentary conditions and seafloor topography. Other knowledge gaps are represented by the influence of the initial effective stress conditions, nucleation process, thresholds of slope angle, evolution of spreading, and run out dynamics.

This study addresses the following research questions: i) What is the global distribution of subaqueous spreading?; ii) What are the morphological and sedimentological characteristics of subaqueous spreading?; and iii) How do these compare with those of terrestrial spreading?

The approach used in this contribution starts with the compilation of a database of published case studies and a statistical analysis of these records. The literature review used for the compilation of the database suggests the preferred terminology, which is used within this contribution and should be used in future studies for describing subaqueous spreading. This analysis highlights the major physiographic and geological characteristics of subaqueous spreading, the mode of failure, the sediment most commonly involved, and the potential trigger mechanisms. This work also highlights the challenges encountered in defining the general characteristics of this type of mass movement and the lack of common descriptive parameters for identifying subaqueous spreading.

2. Brief overview on terrestrial soil spreading studies

Soil spreading is a phenomenon that has also been widely observed in subaerial settings, where it has been the focus of thorough geotechnical investigations (Youd, 1978, 1995; Terzaghi et al., 1996), in particular along fluvial and coastal plains. Within this study, spreading landslides in subaerial conditions are classified into two sub-groups: 1) earthquake-related lateral spreading; and 2) quick clay landslides. We focused on these two specific groups because they share similar aspects with subaqueous spreading as it will be highlighted in Section 5.4 of the discussion, and we will leave rock spreading out of this classification.

2.1. Earthquake-related lateral spreading

Earthquake-related lateral spreading occurs on gently inclined slopes ($< 6^{\circ}$ Durante and Rathje, 2021), along waterlines, and in water bodies that are predominantly characterized by fine grained, sandy or silty sands, which are Late Pleistocene or Holocene in age. These sediments are un- or poorly consolidated, and can undergo liquefaction when under undrained conditions and following cyclic loading (sensu

Terzaghi et al., 1996). When this happens, the sediment loses its frictional resistance and behaves like a liquid, with the consequence that it travels upwards, exploiting fractures and openings in the upper stratigraphic layers, and venting the elutriated sediment at the surface. Historically, spreading is a type of mass transport that has been associated with earthquakes. Earthquake-related lateral spreading has received the attention of the geological and geotechnical communities, particularly since the Mw 8.51964 Alaska and Mw 7.5 Niigata earthquakes events (Wallace, 1965; Kawakami and Asada, 1966; McCulloch and Bonilla, 1970; Scott and Zuekerman, 1973), which caused widespread damage to port and bridge infrastructure, with estimated costs of several hundred million USD for the Alaskan earthquake, and 1 billion USD for the Japanese event (cfr. Taboada-Urtuzuastegui and Dobry, 1998) (for a review of lateral spreading cases see Olson and Johnson, 2008; Araujo and Ledezma, 2020). The scale of the costs involved mean that spreading is considered the most damaging type of ground failure related to liquefaction (National Research Council, 1985).

Datasets collected in open-source databases provide an insightful record of the historical seismicity and geotechnical implications related to lateral spreading, and can help to improve the mitigation of earthquake-related liquefaction and lateral spreading events. The GELCH (Great Earthquake Lateral Spread Case History) database (Bunn and Gillins, 2015; Lingwall et al., 2018), related to earthquakes occurring in subduction zones, and the NGL (Next Generation Liquefaction) database (Brandenberg et al., 2020), which aims to collect worldwide data on lateral spreading in terrestrial settings are two databases that combine case studies of lateral spreading in subaerial settings. Spreads are, however, not exclusively related to earthquakes. For example, investigations related to the causes of the 1979 Nice coastal lateral spreading illustrated that monotonic cyclic activity, such as an anomalous tide, can trigger liquefaction and lateral spreading (Kramer and Seed (1988); Seed et al. (1988), and references therein).

2.2. Quick clay landslides

Quick clay landslides (Bjerrum, 1955; Bjerrum et al., 1969), occur in clay deposits that are characterized by an enhanced sensitivity to failure, and either take the form of flows/earthflows or spreads (Geertsema, 2004; Perret et al., 2019). The sensitivity to failure is expressed as a ratio between (1) the reduction in shear strength of clay when undisturbed compared to (2) when it is remolded, at constant water content (Geertsema and Torrance, 2005). Terrestrial sensitive clays are derived from marine clays deposited during the pre-glacial or post-glacial phases. During the post-glacial phase, the interaction between changing land elevations (experiencing isostatic rebound) and rising sea levels caused a cycle of inundation and subsequent re-emergence of certain portions of the continental land masses. Sensitive clays are considered to have been deposited in topographic, water-filled depressions, but especially in marine or at least brackish bodies of water (Lefebvre, 1996; Geertsema, 2004). As the land masses were re-emerging and meteoric water was infiltrating and causing subaerial erosion, the interaction between marine sediment and fresh water caused the leaching of salt from the marine clay, which contributed to the increased strength of the clay. Salinity reduction is thus a key factor resulting in the extra sensitivity of these sensitive clays (Updike et al., 1988; Lefebvre, 1996). This has been also inferred in marine investigations where spreading has been inferred in association with freshwater (Paull et al., 2021).

Extensive geotechnical studies have been conducted on clay landslides in the Scandinavian region (Hutchinson, 1965; Gregersen and Loken, 1974; Gregersen, 1981; Grondin and Demers, 1996; Solberg et al., 2007; Solberg et al., 2017; Thakur et al., 2017), North America (Kerr and Milling Drew, 1968; La Rochelle et al., 1970; McCulloch and Bonilla, 1970; Updike et al., 1988; Schwab et al., 2004) and New Zealand (Moon et al., 2013; Lowe et al., 2017), where sensitive clay was also observed. For example, in North America, the last glaciation (from 12.5 to 10 kyr BP) covered most of Canada, part of the northern US and part of Alaska, with the most extensive post-glacial marine clay deposits in the Ottawa Valley-St Lawrence Lowlands covered by the deposits of the Champlain Sea (Lefebvre, 1996; Brooks and Aylsorth, 2011), known also as 'Leda Clay' (Gadd, 1975). These deposits have been affected by numerous clay landslides (Locat et al., 2015; Demers et al., 2017; Locat et al., 2017; Tremblay-Auger et al., 2020), with a typical spreading morphological 'thumbprint-like pattern' as recognized in aerial images by several authors (Mollard and Hughes, 1973; Quinn et al., 2011; Demers et al., 2014; Demers et al., 2017). A catalog of the clay landslides observed in the area of Ottawa is a good representation of this type of landslide (Brooks and Crow, 2020).

Similarly, clay landslides can also occur in riverbank deposits and, in some cases, also occupy meandering rivers. They occur on surfaces with a slope ranging between 5 and 20 degrees (Dey et al., 2015) and their aerial extent varies from 0.5 km^2 to a few squared kilometers. The horsts and grabens that form in these sensitive clay landslides are characterized by clay- to silty clay- and often exhibit horizontal stratigraphy inside the blocks (Locat et al., 2017). The mode of failure of clay landslides is typically retrogressive (or progressive upslope), but some examples have also shown that the blocks appear to have undergone significant translation (detachment type) (Updike et al., 1988; Tremblay-Auger et al., 2020). This is in agreement with evidence of spreading at the Træ-nadjupet Slide, offshore Norway, where detached sediment ridges were described as the morphological effect of the rotational back-tilting mechanism of failure (Laberg and Vorren, 2000). The driving process for a clay landslide is often associated with toe erosion, due to the fact that most of them are located along meandering rivers (Brooks and Crow, 2020), but the speculated trigger mechanism is typically attributed to climatic causes, anthropogenic work, or in some cases also to seismic loading (Aylsworth and Lawrence, 2003; Brooks, 2013). In addition, modelling attempts have also shown that groundwater seepage could induce shear stress in highly sensitive clay (Wang et al., 2021).

3. Methods

3.1. Design of the subaqueous spreading database

The subaqueous spreading database ('*SubSpread*') was built on the basis of the guidelines provided by Clare et al. (2018) for the morphometric description of subaqueous landslides. We incorporated case studies from literature, considering all the available papers about subaqueous landslides (126 research articles) and the review studies in the volume of books 'Submarine mass movements and their consequences' from 2003 up to 2020, for building a database as complete as possible. We followed the morphological definition of spreading as detailed by Varnes (1978) and its successive updates (Cruden and Varnes, 1996; Hungr et al., 2014), along with the topographic description in Micallef et al. (2007). Where no detailed description or clear classification of the landslides (or areas thereof) as spreads was provided in the manuscript, we studied the bathymetric maps or the seismic profiles provided to find unequivocal evidence of geomorphic features of spreading (e.g. ridges and troughs, often also mentioned in aerial view as 'stairs', or 'step-stair morphology'). In this contribution, we use the term 'subaqueous spreading' to incorporate spreading events observed in both lacustrine and marine systems, and we omit the adjective 'lateral', which is mainly associated with spreading on land and liquefaction following an earthquake (discussed in Section 2.1). The word 'creeping' is not used here to define spreading. Creeping refers to slow or extremely slow movements that occur on some landslide bodies, and thus does not identify any specific morphology (Varnes, 1978).

We were not always able to find all the information required for our database, so we have ranked our entries on the basis of the data available (Huhnerbach and Masson, 2004), and designed the statistical analysis in light of these limitations. In some case studies, spreading was the only type of mass movement identified (e.g. spreading observed in Malta; Micallef et al., 2016; Capo Vaticano Landslides, South Tyrrhenian Sea,

Casalbore et al., 2018; cases of spreading at Lake Tekapo, New Zealand, Mountjoy et al., 2018; Licosa Landslide, South Tyrrhenian Sea Sammartini et al., 2018). In other cases, spreading characterized only a portion of the entire landslide complex area. This is observed on the landslides occurring offshore Norway (Traenadjupet slide, Laberg and Vorren, 2000; Nik Slide, Lindberg et al., 2004; Tampen Landslide, Barrett et al., 2020), but also on the eastern Canadian continental margin (Normandeau et al., 2018), and on the Sahara Landslide, Northwest Africa (Li et al., 2016). For the latter, the proportion of spreading is incorporated into the database, along with a description of the main landslide body (Fig. 1). The geographic, physiographic and geological parameters included in the database give information about the entire landslide (or landslide complex) where spreading is observed, even if the extent of the spreading does not cover the entire landslide body. The physiographic parameters are reported from the cited literature.

The database organization and its categories are shown in Fig. 1. A description of each category can be found in the Data Supplement.

3.2. Classification of the database entries

The information collected for this Database (DB) was not always complete and exhaustive. We thus introduced a ranking system that provides information about the quality and completeness of each specific DB record. The entries are ranked from 1 to 5, as detailed in Table 1.

3.3. Quantitative analysis

We used Spearman's rank correlation to quantitatively assess any potential correlations between parameters (Table 4DS). Spearman's correlation is used to find correlations between non-linear and highly skewed datasets, such as ours. Spearman's correlation coefficient (ρ) is based on ranked values for each variable, and is defined by the following equation (Rees, 2000):

$$\rho = 1 - \frac{6\sum d_i^2}{n(n^2-1)}$$

where d_i is the difference between the two ranks of the observations and n denotes the number of observations. In order to calculate the Spearman's coefficient, we ranked the values of each variable chosen for the correlation based on the range of values characterizing each of them. The array resulting from this first step was used to calculate Spearman's correlation coefficient (ρ) in excel (Glen, 2021). We also calculated the corresponding degree of freedom, t values and p values for each correlation pair to estimate the significance of the correlation. We calculated Spearman's correlation for the following parameters referring to the entire landslides showing spreading: slope, length, area, thickness, and Skempton ratio. The Skempton ratio is defined as the ratio between the depth of the displaced mass (i.e. the thickness, D) and the total length of the displaced material, L (Table 3DS). The thickness was, in most cases, available as a range of values (e.g. between 20 and 44 m, for the Storegga Slide, Micallef et al., 2007), and we used the maximum value of thickness for those case studies. When possible, individual morphometric parameters were extrapolated for each landslide characterizing landslide complexes (Greene et al., 2006; Lastras et al., 2006) It was not possible to calculate the same statistics just for the area where spreading was observed, because the morphometric parameters exclusively related to the process of spreading were lacking for most of the manuscripts reviewed for this study.

4. Results

4.1. Consistency of the datasets available in the literature

Reporting of subaqueous spreading largely relies on fragmented information that is often qualitative and/or not exhaustive enough for morphometric analysis. Nonetheless, we identified 32 case studies where spreading was unequivocally observed or reported (Fig. 2). The type of information that is most commonly available is the following: geographic location (100 %), depositional setting (94 %), area occupied by the slide (75 %), and slope angle (81 %) measured at the headwall or in the depositional area of the landslide. Geological information about the type of material involved in the sliding and mode of failure are also amongst the most commonly available pieces of information (84 % and 65 % respectively). The speculated trigger mechanism is often included (88 %), while volume and thickness of the slide are commonly not quoted (56 % and 44 %, respectively). Geotechnical tests (31 %), evidence of overpressure, and gas fields (both 34 %) are only reported for nearly one third of our case studies. Although ridges and troughs are distinctive topographic markers of spreading (Micallef et al., 2007), few contributions quantitatively reported these features and their attributes. Contrastingly, 97 % of our case studies include a qualitative description of the spreading morphology. The absolute values and the frequency of the database categories and subcategories considered in our study are summarized in Table 2. Only 13 of the 29 total DB categories or subcategories included in our DB are filled by at least 50 % of the case studies.

The cases of subaqueous spreading that have been collected so far are biased by the areas where more scientific research in relation to exploitation of geo-resources has been conducted, i.e. the northern hemisphere, in particular the Norwegian and North American margins. This is true also for the seismic resolution used to image the stratigraphy of the ridges, whenever observed (Greene et al., 2006; Lastras et al., 2006; Baeten et al., 2013; Barrett et al., 2020).

4.2. Spatial distribution of subaqueous spreading

The case studies recorded in the database 'SubSpread' include a higher number of spreading cases along passive margins (20) compared to on active margins (12) (Fig. 2). Amongst the 21 case studies found along passive margins, 8 are in Norway (6 of them in the Norwegian Sea), and 7 are located offshore Canada and the US. Subaqueous spreading along active margins is observed in and offshore New Zealand (2 cases), offshore California (3 cases) and in the Mediterranean region (7 cases). Although the higher concentration of spreading cases in regions where more research on subaqueous landslides has been carried out highlights a sampling bias for the information so far available in our DB, this finding still reveals a link between the occurrence of spreading and setting, with passive glacial continental margins, where glaciomarine clays were deposited, showing a higher incidence of spreading.

4.3. Setting and topographic characteristics

Subaqueous spreading is predominantly observed on the continental slope (38 % of the case studies) and continental shelf (31 %). The remainder of the case studies are distributed between the shelf break (6.3 %), river deltas (6.3 %), fjords (6.3 %) and lake deposits (9 %).[1]

The topographic characteristics of mass transport deposits with some component of spreading vary significantly. The downslope length for landslides with spreading varies notably from 0.4 km (Wabush Lake, Labrador, Canada) to a maximum value of 900 km (Sahara landslide complex, Fig. 1DS, in the Data Supplement). Likewise, the area and volume of landslides with spreading morphology is highly skewed, with a few landslides that are characterized by a very large areal extent and many smaller landslides (Fig. 2DS). For representation purposes, we separate the areas of these landslides into three groups: landslides with an area smaller than 10 km^2; landslides that have an area between 10

[1] Note the total does not make up to 100 % because only the 93 % of the records considered in 'SubSpread' reported information about the 'setting' (Table 2).

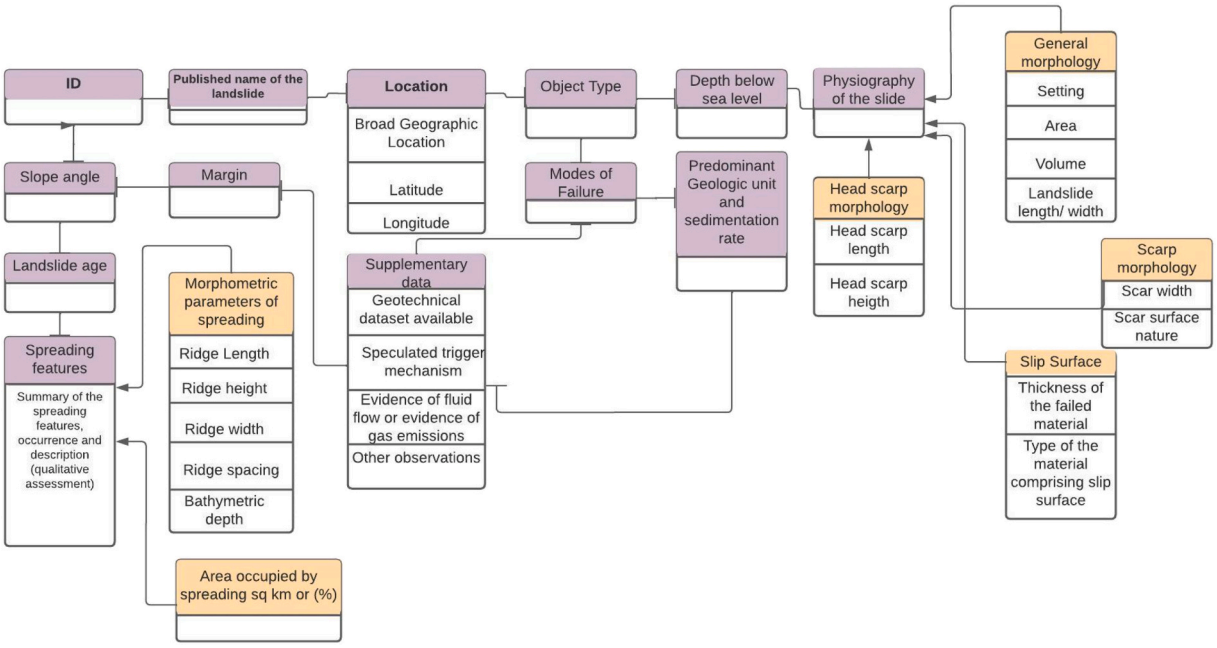

Fig. 1. Hierarchical organization of the Database 'SubSpread'. Each rectangular shape shows the Database categories (purple) with related subcategories (orange) and table fields. A detailed description of each category, subcategory and table field can be found in the Data Supplement (The Database categories). (For interpretation of the references to colour in this figure legend, the reader is referred to the web version of this article.)

Table 1
Description of the ranking system used for classifying the entries contained within our DB 'SubSpread'.

Ranking	Description
1	• All introductory DB categories, including location, depth and MTD/ MTDC classification are filled • At least 3 table fields under 'General morphology' are populated or all the fields relevant for quantitative analysis (such as length, area, volume, and thickness) are populated • Slope angle is described • Geology of the area and sedimentation, landslide age, scar morphology and headscarp morphology are populated • Spreading features are both qualitatively and quantitative described • The supplementary fields (especially regarding geotechnical information) is generally complete
2	• The DB subcategory 'General morphology' is populated • Relevant information for statistical analysis such as thickness, volume or width is lacking • A qualitative description of spreading features is provided but the morphometric parameters are not always reported
3	• The introductory DB categories are all populated • The DB category 'Physiography of the slide' is not consistently populated • Parameters used for statistical analysis are missing or not consistently reported (for example, length of the deposit, area of the deposit, slope angle, thickness of the deposit, see Data Supplement 'The Database, (DB) categories) • The qualitative description of the spreading morphology is not very detailed and a quantitative description of the features characterizing the spreading morphology is absent
4	• Spreading is mentioned in the cited manuscript but a clear representation of it is not available

and 1000 km^2; and landslides with areal extent >1000 km^2 (Fig. 2DS). The landslides belonging to the largest group are the Big 95 Debris Flow (2000 km^2), the Nyk Slide (2200 km^2), the Traenadjupet Slide (9100 km^2), the landslides on the Laurentian fan on the Eastern Canada (totaling 14,000 km^2), the Sahara Slide (48,000 km^2), the Tampen Slide (>48,000 km^2), and the Storegga Slide (95,000 km^2). The Norwegian slides, where spreading is commonly observed, represent a group of mass transport deposits that are consistently characterized by a large aerial extent and volume.

It is possible to estimate the percentage of the aerial extent of the landslide or landslide complex that is dominated by spreading morphology from the images available for 24 case studies (of the 33 available) (Table 1DS). A quantitative estimation of the spreading morphology was possible only in 9 case studies. Some of the giant landslide complexes such as Storegga, Tampen or Sahara landslides are characterized by a comparatively small percentage of their area comprising spreading morphology from 3 % up to ~30 %. For example, the total area covered by spreading on the Tampen Slide is ~1720 km^2, which is <3.6 % of the total area of the slide; Barrett et al., 2020). In contrast, for smaller landslides (e.g. the Lake Tekapo[2] landslide in New Zealand or the Licosa landslide in the Tyrrhenian Sea), spreading morphology (ridges and troughs) typically affects an area > 30 % of the landslide area, up to 60 % or more (spreading observed offshore Malta, Micallef et al., 2016; case studies of Capo Vaticano Landslide Complex, Casalbore et al., 2018). An example of the different coverage of spreading morphology is shown in Fig. 3.

With the type of datasets available so far, it is not possible to estimate the links between the area covered by spreading morphology, which infers spreading failure, and the entire landslide body; in particular for those large landslides where the depositional area results from multiple failure events, or where spreading may have occurred subsequent to the main failure (Micallef et al., 2009; Mountjoy et al., 2009; Li et al., 2016; Barrett et al., 2020). This research has shown a link between some of the largest subaqueous landslides and spreading. However, the kinematics of failure and of how spreading has influenced subsequent catastrophic failure cannot be constrained with the current dataset. This will be further addressed by modelling studies.

We classify three ranges of slope gradient for the instances of spreading documented by the case studies we analyzed: equal to or <1° (10 case studies); between 1 and 3° (14 case studies); and >3° (6 landslide bodies) (Table 2DS). The landslides characterized by spreading

[2] The area covered by spreading in subaqueous landslides at Lake Tekapo was not reported in the paper (Mountjoy et al., 2018) considered in the DB, but from a dataset available to the authors.

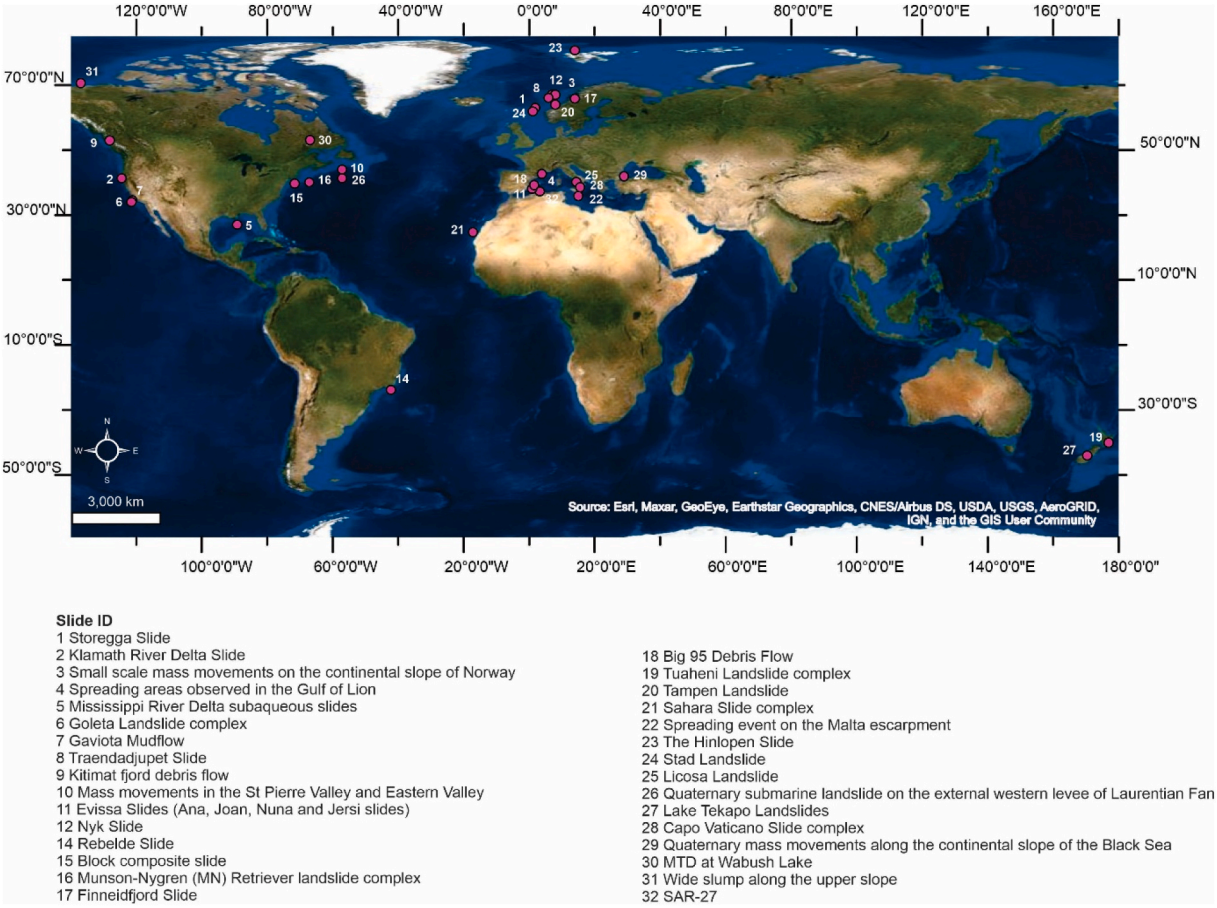

Fig. 2. Map of subaqueous spreading case studies included in our database and their geographic distribution. Each landslide listed in the database is characterized by an ID number and a broad geographic location. The numbering shown in this figure corresponds with the ID used in the 'SubSpread' DB. Please note n. 13 is not shown on this map because this record in the DB represents a review paper.

tend to have a very long run-out distance in comparison to the thickness of the material that failed. Consequently, the Skempton ratio (D/L) is small for all the cases, ranging between 0.05 and 6.5 $\times$ 10^{-3} (Table 3DS). The values of the Skempton ratio were only calculated for 12 cases due to a lack of information for the other studies.

The quantities of slope, length, area and thickness were taken into consideration for the correlation analysis (Table 4DS). There is a weak negative correlation between slope angle and length (Spearman's rank correlation, $\rho = -0.49$) and between the values of slope angle and area ($\rho = -0.31$), but a weak positive correlation ($\rho = 0.35$) between thickness and area, and a very strong positive correlation between the length and the area of the slope deposit ($\rho = 0.87$). Length and area tend to increase as the slope angle decreases, but this correlation is moderate. These results are consistent with the findings from the Skempton ratio stated above, which indicate that the landslides or landslide complexes characterized by spreading generally have a very low angle but a large areal extent.

5. Discussions

5.1. Defining spreading morphology

Spreading morphology is described with different terminologies; however, despite being the diagnostic criteria of the process of spreading, the reviewed manuscripts often do not provide substantial information about the morphometry of the spreading. In addition, the characteristics summarized here as being indicative of subaqueous spreading are exclusively related to the case studies collected in our database (i.e. to the literature so far available), and thus there is an implicit sampling bias.

We propose that spreading is broadly described as having an irregular hummocky topography, with tensional transversal structures and a distinctive staircase morphology, in some cases identified as rotational slumps (Coleman and Prior, 1978; Prior and Coleman, 1978; Paull et al., 2021) or otherwise recognized as ridges. Ridges and troughs, or terraces, are often parallel or subparallel to the headwalls and are typically perpendicular to the direction of movement of the main mass transport. Both the ridge length and height are usually in the order of a few decameters to a few hundred meters (Table 3). Spreading ridges appear closely spaced near the headwall of the slide, but this spacing expands downslope. The internal stratigraphy of the ridges is preserved in some cases, but in others is chaotic with acoustically transparent units (Greene et al., 2006; Lastras et al., 2006; Baeten et al., 2013; Baeten et al., 2015; Normandeau et al., 2018; Barrett et al., 2020; Paull et al., 2021). This suggests that the internal layering of these features has been plastically deformed. The occurrence of fluid-injections, sand boils and mud volcanoes is often documented adjacent to mass transport deposits with spreading morphology, or even in between the ridges (Coleman and Prior, 1978; Prior and Coleman, 1978; Field et al., 1982; Paull et al., 2021; Wu et al., 2021). A morphological and morphometric description of spreading is needed in order to distinguish this process from other topographic features that resemble ridge and trough morphology, in bathymetric view or in seismic interpretations, as happened with a

Table 2
Availability of data for all of the DB categories in 'SubSpread'. Refer to Fig. 1 and to the Data Supplement for more details about the DB categories and explanation of the subcategories.

DB Categories[(1)]/Subcategories[(2)]	No Info	Records available	% records available (from 32 case studies)
Location[(1)]	0	32	100.0
Object type[(1)]	0	32	100.0
Depth below sea level [(1)]	6	26	81.3
Setting [(2)]	2	30	93.8
Area[(2)]	8	24	75.0
Volume[(2)]	14	18	56.2
Landslide length[(2)]	10	25	78.1
Landslide width[(2)]	20	12	37.5
Headscarp length[(2)]	26	6	18.7
Headscarp height[(2)]	15	17	53.1
Scar width[(2)]	25	8	25
Scar surface nature[(2)]	22	11	34.3
Thickness of material comprising slip surface[(2)]	19	14	43.8
Slope angle[(1)]	6	26	81.3
Landslide age[(1)]	17	16	50.0
Margin type[(1)]	0	32	100.0
Mode(s) of failure[(1)]	11	21	65.6
Predominant Geological Units[(1)]	5	27	84.8
Summary of spreading features[(1)]	1	32	96.8
Ridge length[(2)]	18	14	43.7
Ridge height[(2)]	18	14	43.7
Ridge width[(2)]	28	4	12.5
Ridge Spacing [(2)]	25	8	25
Depth of ridges (below sea level) [(2)]	27	5	15.6
Area occupied by spreading km^2 or % [(2)]	28	4	12.5
Geotechnical data available [(2)]	22	10	31.3
Speculated trigger mechanism [(2)]	4	28	87.5
Evidence for fluid flow and overpressure or evidence of gas emissions [(2)]	21	11	34.4

sediment wave field on the Adriatic sea (Berndt et al., 2006), or on what was known as 'The Kidnapper Slide' (Barnes and Lewis, 1991), which was later acknowledged as a dune field,[3] or to a repetitive pattern of 'cyclic steps' as identified by Bellwald et al. (2015) and Hughes Clarke et al. (2014), described as sediment bedform migration.

Some contributions describe spreading as small- or large scale 'rotational slumps' (Prior and Coleman, 1978; Barnes and Lewis, 1991; Piper et al., 1999; Paull et al., 2021). Slumps are closely related to spreading features because their driving force is represented by a small gravitational force acting on liquefied or partially liquefied fine-grained material over a sub-horizontal surface (Strachan, 2004; Strachan and Alsop, 2006). Slump bodies move because of the liquefaction of the glide plane, and are identified as rotational mass movements (in contrast, Cruden and Varnes, 1996 encouraged the replacement of the term 'slump' with rotational slides) – both characteristics that are commonly attributed to the spreading process too. However, in contrast to spreading, slumps show more consistently plastic deformation inside these blocks, with soft sediment deformation being recorded in both recent and fossil examples onshore (Spalluto et al., 2007; Alsop and Marco, 2011; Morsilli and Moretti, 2011). More importantly, slump bodies do not show the extensional downslope morphology and, thus, ridges and troughs that are associated with spreading.

5.2. *Mode of failure, material involved in the failure, and preconditioning factors*

Most of the landslides and landslide complexes with spreading morphology seem to have failed retrogressively. However, several studies clearly state that this morphology could be explained by a combination of translational and retrogressive failure (translational retrogression) (Coleman and Prior, 1978; Prior and Coleman, 1978; Barnes and Lewis, 1991; Piper et al., 1999; Vanneste et al., 2006; Baeten et al., 2013; Li et al., 2016). Mulder and Cochonat (1996) used the Skempton Ratio to distinguish between translational [$\leq$ 0.15] and rotational slides [0.15–0.33]. This classification did not consider spreading as a type of offshore mass movement. The values of the Skempton Ratio calculated for the landslides affected by spreading morphology presented in this contribution (Table 4DS) are far smaller than the thresholds suggested by the classification of Mulder and Cochonat (1996). Our dataset cannot address the complex links between retrogressive and translational failure modes for explaining the large aerial extent of the landslides with spreading morphology. This will need to be investigated in the future using a finite element modelling simulation.

We find that very fine grained deposits (clay material with a silty component, or silt and silty sands) characterize the materials that failed in all the case studies considered in our DB. Areas where spreading is prevalent tend to be associated with Quaternary sediments from glacial till, glaciogenic deposits, or muddy sedimentary deposits overlain by a Holocene hemipelagic succession. Contourites and their geological contrast with glacial sediments also seem to play an important role in the development of spreading (Laberg et al., 2002; Lindberg et al., 2004; Micallef et al., 2007; Ashabranner et al., 2010; Baeten et al., 2013; Baeten et al., 2015). Contourites result from constant sedimentation driven by water currents at intermediate or deeper water depth. Glaciogenic debris flows occur due to sediment discharge from glacial bodies at the continental shelf and, therefore, mainly occur during glacial periods. Contourites, which occur during interglacial times, thus fill in the surface of slopes, replacing the material excavated by the glaciogenic debris flows (Gatter et al., 2020). These inter-layered glaciogenic debris flows and contourites are frequently affected by slope failures, as evidenced by the Nyk Slide and other slides on the continental margin offshore Norway (e.g. the Storegga, Trænadjupet and Sklinnadjupet slides), which has been affected by multiple sliding events in the past (Evans et al., 2005; Barrett et al., 2020; Batchelor et al., 2021). Hence, the occurrence of large cyclic sliding events should not be considered as a rare event (Bryn et al., 2005). Extensive geological and geotechnical work conducted in the headwall area of the Storegga Slide complex has shown that the contouritic sediments here have a distinctive high clay content, water content, plasticity, and liquidity index. All of these result in the contourites being of lower strength, and thus of higher sensitivity, than the glacial debris sediments (Kvalstad et al., 2005; Baeten et al., 2013). These physical characteristics predispose the contouritic sediment to be more susceptible to softening or liquefaction. These studies also reveal that the Norwegian continental slope is composed of a sequence of glaciomarine sediments interlayered with hemipelagic and contouritic sediments (Laberg and Camerlenghi, 2008). The regular deposition of well sorted, fine-grained contouritic sediments during interglacial intervals on slopes may thus represent a preconditioning factor for recurring slope failure at the same site over an extended period of time (even glacial/interglacial cycles) (Hogan et al., 2016; Gatter et al., 2020).

Sandier contourite systems could also act as detachment surfaces for the slide (Prior et al., 1982; Nouguès et al., 2009); for example, at the Tuaheni landslide complex, where evidence of sandier bodies embedded in the glide plane has been found (Carey et al., 2019; Crutchley et al., 2022). When sand is involved in the failure, the equilibrium is likely altered by the liquefaction of the sediment bodies following seismic shaking (Wilson et al., 2004). The mud/sand transition is a product of the climatic cyclicity, as the sandy layers are deposited during interglacial periods by relatively stronger bottom currents. Contouritic sediments were also inferred to be on the continental slope immediately adjacent to the Hinlopen Slide, a giant submarine landslide in the Arctic Ocean (Vanneste et al., 2006). Other cases have been presented from the

[3] Mountjoy, J.2022 personal comm.

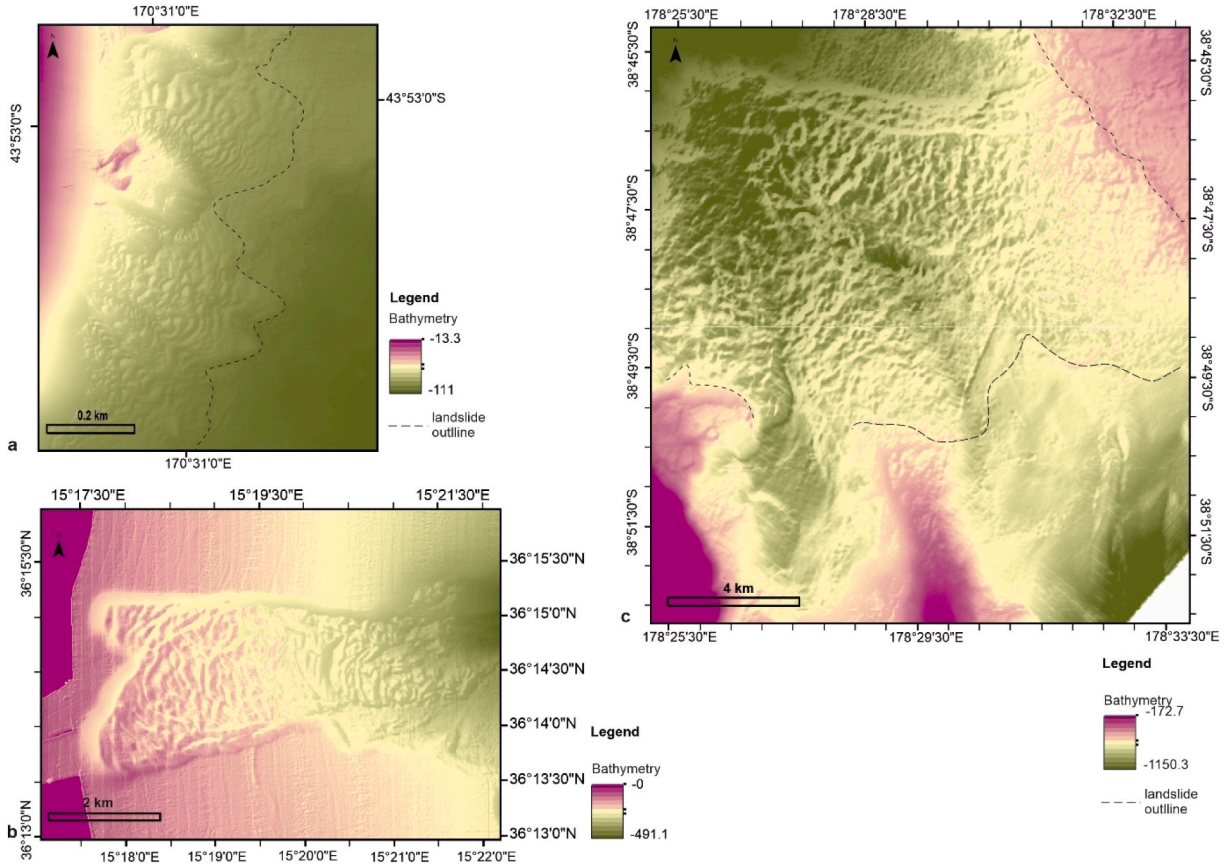

Fig. 3. Spreading types and coverage at three different case studies: a) on the Malta escarpment (Micallef et al., 2016); b) Tuaheni landslide complex, TLC, (Mountjoy et al., 2009); c) Lake Tekapo landslide (Mountjoy et al., 2018). The Malta escarpment and Lake Tekapo slides are examples of spreading where the spreading morphology covers most of the aerial extent of the slide. This is less clear at the TLC, which is a much wider landslide (see Fig. 1DS) where spreading morphology occupies ~30–40 % of the landslide extent.

Table 3
Summary of the major physiographic parameters that describe the landslides and landslide complexes with spreading morphology in our DB.

	Landslide length (km)	Landslide area (km^2)	Slope Angle (degrees)	Thickness of the failed deposit (m)	Skempton ratio ($x10^{-3}$)	Ridge length	Ridge height
Range of values	0.4–900	0.76–95,000	$1 \leq x \leq 3$	4–140	0.05–6.5	~hundreds of meters, from a few meters up to km	From a few meters up to tens of meters

NW Atlantic Margin; for example, the spreading landslides offshore eastern US and Canada are also influenced by the deposition of sediment drifts on the Labrador Shelf. These sediments are the product of the progression of glacial sediment to the shelf break and the subsequent feeding of the deep water basin current with these glacially-derived sediments (Piper, 2005). The same slope morphology has influenced the distribution of the contourites, which are thickest in the slope embayment. In particular, the negative curvature of a contourite drift is also considered a preconditioning factor for failure (Miramontes et al., 2018).

The statistics calculated from our database and reported in section 3.3 reveal that the aerial extent of subaqueous mass transport deposits that include areas of spreading varies widely; however, these landslides are typically characterized by a very large aerial extent in comparison to the thickness of the material that failed (i.e. have a very small Skempton Ratio; especially for the largest landslide complexes, Table 3DS). This can be explained by the long run-out that occurs when the failing sediment undergoes a loss of shear strength, which is linked to liquefaction or softening (Locat and Lee, 2002). Contourites and glaciogenic deposits are unconsolidated, and when in undrained conditions (with higher pore water pressure), sediment bodies are less dense than in the appropriate steady state condition, therefore sediment is more likely to flow in comparison to the same type of sediment in steady state condition (Locat and Lee, 2002; Rebesco et al., 2014). During subaqueous failure - in cases where there is rapid sediment deposition, gas breaching through, or exogenic trigger mechanisms (earthquakes) - the sediment can fail rapidly (Locat and Lee, 2002). This may, at least partly, explain why some of the largest subaqueous landslides involve contouritic sediment and have a very long run-out despite being on gentle slopes.

In contrast to the Norwegian margin, the isolated spreading episodes occurring within other large landslides (e.g. the Sahara landslide or the landslides in the Santa Barbara Basin) are caused by site-specific conditions such as sedimentation-controlled processes (shown by numerical modelling of the landslides observed in the Santa Barbara Basin; (Stoecklin et al., 2017) or local tectonic activity (assumed for the giant Sahara landslide; (Li et al., 2016).

5.3. *Trigger mechanisms of subaqueous spreading*

Seismic loading is inferred to be the major trigger mechanism for subaqueous spreading for most of the case studies included in our database (Field et al., 1982; Piper et al., 1999; Micallef et al., 2007;

Nouguès et al., 2009; Li et al., 2016; Casalbore et al., 2018; Normandeau et al., 2018; Paull et al., 2021). In some cases, multiple endogenic preconditioning factors, such as over-sedimentation and toe erosion, were supplemented by seismic loading, cumulatively resulting in spreading (Coleman and Prior, 1978; Prior and Coleman, 1978; Prior et al., 1982; Laberg et al., 2002; Lindberg et al., 2004; Mountjoy et al., 2009; Ogata et al., 2014; Micallef et al., 2016; Normandeau et al., 2018; Sammartini et al., 2018; Barrett et al., 2020). Interestingly, the landslides characterized by spreading morphology seem to be more concentrated along passive margins that have low tectonic activity (Laberg and Vorren, 2000; Laberg et al., 2001; Lindberg et al., 2004; Micallef et al., 2007; Chaytor et al., 2011; Baeten et al., 2013; Hjelstuen and Grinde, 2015; Normandeau et al., 2018). Most of the case studies, as generally, other types of subaqueous landslides, lack geotechnical measurements and paleoseismic investigations that could corroborate the authors' assumptions about trigger mechanisms or potential seismogenic sources. However, a conspicuous number of spreading case studies, and in particular those adjacent to the passive glaciated margins of Canada and the Scandinavian region, infer that the seismic loading hypothesized to be the main trigger mechanism is a consequence of isostatic rebound (Adams, 1989; Arvidsson, 1996; van Loon et al., 2016; Pisarska-Jamroży and Woźniak, 2019). This association warrants further investigation, particularly in light of recent paleoseismic studies in glaciated margin areas (Steffen et al., 2021, and references therein), which confirm that earthquakes and earthquake sequences onshore occur as a consequence of glacial uplift.

5.4. How similar are subaqueous and subaerial soil spreads?

The wealth of geotechnical dataset characterizing terrestrial soil spreading made possible to advance model and hazards implications of this mass transport (see Giona Bucci and Tuttle, 2021, and references therein). This is not the case for subaqueous spreading which often lacks detailed sedimentological and geotechnical analysis, as showed in this contribution, and causing specific numerical modelling simulations to be more challenging. However, subaqueous and subaerial soil spreading have several aspects in common. Horst and graben structures are particularly visible in clay landslides, where they tend to characterize the whole sediment body and have an average size of tens of meters (Prior et al., 1982; Piper et al., 1999; Lindberg et al., 2004; Lastras et al., 2006; Micallef et al., 2007; Baeten et al., 2013; Hjelstuen and Grinde, 2015; Micallef et al., 2016). These ridges can, however, be larger (e.g. the Tampen Slide (Barrett et al., 2020) where ridges of ~120 m are observed) or smaller (<5 m high; Lastras et al., 2003; Casalbore et al., 2018; Paull et al., 2021). These characteristic features are less visible in earthquake-related lateral spreading, where deep fractures indicate the incipient formation of topographic depressions (grabens), but their overall displacement does not exceed decimeter-scale, or is of the order of meter-scale (Seed et al., 1985; Holzer, 1998; Tinsley et al., 1998; Cetin et al., 2004; Cubrinovski et al., 2010). Ridges and troughs resulting from subaqueous spreading are similar to the spreading morphology observed in clay landslides, although ridges in the subaqueous setting are often larger in scale. The detached blocks experience minimum translation (from decameters up to a few meters), and minimum internal deformation is identified in the clay landslides. This is not always the case for subaqueous spreading where, in some cases, it is possible to observe transparent chaotic acoustic facies that are indicative of plastic deformation, even in high-resolution seismic data (Greene et al., 2006; Lastras et al., 2006; Baeten et al., 2013; Normandeau et al., 2018; Barrett et al., 2020; Paull et al., 2021).

Onshore, the extent of clay landslides and earthquake-related lateral spreading is often confined to areas adjacent to meandering rivers (Tuttle and Barstow, 1996; Caputo et al., 2012; Cubrinovski and Robinson, 2016; De Pascale et al., 2016; Brooks and Crow, 2020). In comparison, the aerial extent of subaqueous landslides affected by spreading morphology can be thousands of squared kilometers for the largest slides; e.g. Traenadjupet (9100 km^2), Sahara Slide (48,000 km^2), or Storegga Slide (95,000 km^2), even though the spreading morphology affects a smaller percentage of the aerial extent of these landslides (up to 50 % for the Traenadjupet Slide, ~30 % for the Sahara Slide, and up to 25 % for the Storegga slide; Table 1DS). The link between spreading morphology and long-runout distance, in association with some of the largest landslides observed, warrants further research that only modelling simulations can solve.

In a terrestrial setting, the trigger mechanism for clay landslides and earthquake-related lateral spreading is often unequivocally identified. Furthermore, radiocarbon dating enables researchers to date and link this type of mass movement to historically documented earthquakes. In the subaqueous setting, however, constraining both the age and the trigger mechanism is typically more complicated due to burial and erosional processes, as well as the ease of access for sampling. However, recent geotechnical investigations (e.g. Carey et al. (2019, 2022), coupled with geophysical and sedimentological interpretation (Crutchley et al., 2022), suggest that a long duration high amplitude earthquake could lead to significant episodic movement on gently inclined surfaces. Within this framework, and given that terrestrial soil spreading is a costly landslide hazard (see Section 2.1), subaqueous spreading might represent an important seafloor hazard too. Table 4 provides a compendium of the major geological characteristics shared amongst the different spreads elucidated in this contribution with a particular emphasis on subaqueous spreading.

6. Conclusions

We identified thirty two cases of subaqueous spreading and compiled their information in a database. Despite being aware that the research studies so far considered are biased towards areas that are characterized by more research or sub-seafloor exploration and exploitation of georesources, a cluster of these features is concentrated in the peri-glacial settings of the Norwegian and Canadian shelfs. Other cases of considerable size have also been identified in the Mediterranean region, along the Santa Barbara channel, both in and offshore New Zealand, and on the West African margin. Subaqueous spreading is an extensional type of movement, which is driven by strain softening of clays or liquefaction of sandy layers interlayered with silty or muddy layers, on quasi-horizontal or gently inclined surfaces (typically <3°). Spreading morphology generally either constitutes a minor component of a large landslide complex (<30 % of the total surface area), or is a predominant feature of a smaller landslide. Its unique morphological features have been described as a repetitive pattern of topographic highs and lows (ridges and troughs) that are mostly concentrated in the uppermost (extensional) portion of the landslide body, and are less continuous downslope. The acoustic facies of spreading is characterized either by continuous layering of high amplitude reflectors overlying a transparent surface, or as a chaotic seismic facies that suggests internal plastic deformation.

Our analysis shows that contourite deposits, interbedded with glaciogenic and periglacial sediments, play a key role in the susceptibility of the largest submarine landslides to spreading. Contourites are particularly susceptible to failure because they are deposited by constant ocean surficial or bottom currents on very gentle slopes and have a very well sorted grain size. Well sorted sediments tend to be more permeable and thus have a higher water content, which, in turn, favors failure when shear stress is applied.

Subaqueous and terrestrial spreading have similar morphology and driving forces; however, the aerial extent of subaqueous spreading greatly exceeds that of any terrestrial case studies. This is a consequence of the type of sediment involved in the subaqueous spreading (contourites interlayered with glacial sediments). Similarly, to terrestrial spreading, seismic loading appears to be the most common trigger mechanism attributed to subaqueous spreading too, although lacking direct observation, as often occurs for subaqueous landslides, this assumption would require further investigation.

Table 4
Summary of the major characteristics of spreading in terrestrial and subaqueous setting.

Spreads			
	Subaqueous	Earthquake Related	Clay landslides
Slope	0 and 3 degrees	0 and ~ 6 degrees	0 and 20 degrees
Extent	Hundreds of km^2	Hundreds of m^2	Few km^2
Sediment	Clay, silty clay, less commonly sand	Sands, silty sands, silt	Clay, clayey silt, minor presence of sands
Trigger mechanism	Earthquakes (typically suggested to be the main trigger mechanism), cyclic overloading of sediment, isostatic rebound	Earthquakes	Artesian pressure, toe erosion from river, earthquakes
DBs	This contribution	GELCH DB; NGL DB (Lingwall et al., 2018; Brandenberg et al., 2020); and Durante and Rathje (2021)	Brooks and Crow (2020); NADAG DB (Solberg et al., 2017)

Declaration of competing interest

The authors declare that they have no known competing financial interests or personal relationships that could have appeared to influence the work reported in this paper.

Data availability

Data will be made available on request.

Acknowledgments

This research is entirely supported by the Marie Curie action WF-02-2019, under the H2020 program, project number 101003388. The authors are grateful to the Editor who handled our manuscript Prof Achim A. Beylich, and to the reviewers Prof. Christopher Gomez and Prof Mauro Soldati for their comments.

Appendix A. Supplementary data

Supplementary data to this article can be found online at https://doi.org/10.1016/j.geomorph.2022.108397.

References

Adams, J., 1989. Crustal stresses in eastern Canada. In: Gregersen, S., Basham, P.W. (Eds.), Neotectonics And Postglacial Rebound, Volume Earthquakes at North Atlantic Passive Margins. Kluwer Academic Publishers, Dordrecht, pp. 289–297.
Alsop, G.I., Marco, S., 2011. Soft-sediment deformation within seismogenic slumps of the Dead Sea Basin. J. Struct. Geol. 33, 433–457.
Araujo, W., Ledezma, C., 2020. Factors that affect liquefaction-induced lateral spreading in large subduction earthquakes. Appl. Sci. 10, no. 6503.
Arvidsson, R., 1996. Fennoscandian earthquakes: whole crustal rupturing related to postglacial rebound. Science 274 (5288), 744–746.
Ashabranner, L.B., Tripsanas, E.K., Shipp, R.C., 2010. Multi-direction flow in a mass-transport deposit, Santos Basin, offshore Brazil. In: Mosher, D.C.e.a (Ed.), Submarine Mass Movements And Their Consequences, Volume 28. Springer Science+Business Media.
Aylsworth, J.M., Lawrence, D.E., 2003. Earthquake induced landsliding East of Ottawa; a contribution to the Ottawa Valley Landslide Project. In: Proceedings 3rd Canadian Conference on Geotechnique And Natural Hazards, Edmonton, pp. 77–84.
Baeten, N., Laberg, J.S., Forwick, M., Vorren, T.O., Vanneste, M., Forsberg, C.F., Kvalstad, T.J., Ivanov, M., 2013. Morphology and origin of smaller-scale mass movements on the continental slope off northern Norway. Geomorphology 187, 122–134.
Baeten, N., Laberg, J.S., Vanneste, M., Forsberg, C.F., Kvalstad, T.J., Forwick, M., Vorren, T.O., Haflidason, H., 2015. Origin of shallow submarine mass movements and their glide planes—sedimentological and geotechnical analyses from the continental slope off northern Norway. J.Geophys.Res.Earth Surf. 119.
Barnes, P.M., Lewis, K.B., 1991. Sheet slides and rotational failures on a convergent margin: the Kidnappers Slide,New Zealand. Sedimentology 38, 205–221.
Barrett, R.S., Bellwald, B., Talling, P.J., Micallef, A., Gross, F., Berndt, C., Planke, S., Myklebust, R., Krastel, S., 2020. Does retrogression always account for the large volume of submarine megaslides? Evidence to the contrary from the Tampen Slide, Offshore Norway. J. Geophys. Res. Solid Earth 126 p. e2020JB020655.
Batchelor, C.L., Bellwald, B., Planke, S., Ottesen, D., Henriksen, D., Myklebust, R., Johansen, S.E., Dowdeswell, J.A., 2021. Glacial, fluvial and contour-current-derived sedimentation along the northern North Sea margin through the Quaternary. Earth Planet. Sci. Lett. 566, 116966.
Bellwald, B., Hjelstuen, B.O., Sejrup, H.P., Haflidason, H., 2015. Postglacial mass failures in the Inner Hardangerfjorden system, Western Norway. In: Lamarche, G.e.a (Ed.), Submarine Mass Movements And Their Consequences, Volume 41. Springer International Publishing, Switzerland.
Berndt, C., Cattaneo, A., Szuman, M., Trincardi, F., Masson, D., 2006. Sedimentary structures offshore Ortona, Adriatic Sea—deformation or sediment waves? Mar. Geol. 234, 261–270.
Bjerrum, L., 1955. Stability of natural slopes in quick clay. Geotechnique 5, 101–119.
Bjerrum, L., Loken, T., Heiberg, S., Foster, R., 1969. A field study of factors responsible for quick clay slides. In: Proceedings 7th International Conference on Soil Mechanics And Foundation Engineering, Mexico, Volume Stability of natural slopes and embankment foundations. Sociedad Mexicana de Mecanica de Suelos.
Brandenberg, S.J., Zimmaro, P., Stewart, J.P., Kwak, D.Y., Franke, K.W., Moss, R.E., Cetin, K.O., Can, G., Ilgac, M., Stamakatos, J., Weaver, T., Kramer, S., 2020. Next generation liquefaction database. Earthq. Spectra 0, 1–21.
Brooks, G.R., 2013. A massive sensitive clay landslide, Quyon Valley, southwestern Québec, Canada, and evidence for a paleoearthquake triggering mechanism. Quat. Res. 80, 425–434.
Brooks, G.R., Aylsorth, J.M., 2011. Geotechnical characteristics of Champlain Sea Deposits. In: Russel, H.A.J., Brooks, G.R., Cummings, D.I. (Eds.), Deglacial History of the Champlain Sea Basin And Implications for Urbanization; Joint Annual Meeting GAC-MAC-SEG-SGA; May 25-27, 2011; FIeldtrip Guidebook. Natural Resources Canada, Ottawa, Ontario, p. 96.
Brooks, G.R., Crow, H.L., 2020. A guide to landslides in sensitive clay along the north side of the Ottawa River, west of Ottawa-Gatineau, southwestern Quebec. Geol.Surv. Can. 43.
Bryn, P., Berg, K., Forsberg, C.F., Solheim, A., Kvalstad, T.J., 2005. Explaining the Storregga Slide. Mar. Pet. Geol. 22, 11–19.
Bull, S., Cartwright, J.A., Huuse, M., 2009. A review of kinematic indicators from mass transport complexes using 3D seismic data. Mar. Pet. Geol. 26 (7), 1132–1151.
Bunn, M.D., Gillins, D.T., 2015. Assessing lateral spread analysis in areas prone to great and long-duration earthquakes: USGS.122.
Caputo, R., Iordanidou, K., Minarelli, L., Papathanassiou, G., Poli, M.E., Rapti-Caputo, D., Sboras, S., Stefani, M., Zanferrari, A., 2012. Geological evidence of pre-2012 seismic events, Emiliar-Romagna, Italy. Ann.Geophys. 55 (4).
Carey, J.M., Crutchley, G.J., Mountjoy, J.J., Petley, D.N., Saveney, M.J.M., Lyndsell, B., 2019. Slow episodic movement driven by elevated pore-fluid pressures in shallow subaqueous slopes. Geomorphology 329, 99–107.
Carey, J.M., Mountjoy, J.J., Crutchley, G.J., Petley, D.N., Holden, C.F., Kaneko, Y., 2022. Episodic movement of a submarine landslide complex driven by dynamic loading during earthquakes. Geomorphology 408, 108247.
Casalbore, D., Martorelli, E., Bosman, A., Morelli, E., Chiocci, F.L., 2018. In: Society, G. (Ed.), Failure Dynamics of Landslide Scars on the Lower Continental Slope of the Tyrrhenian Calabrian Margin: Insights From an Integrated Morpho-bathymetric And Seismic Analysis, Volume 477, pp. 389–397. London.
Cetin, K.O., Youd, T.L., Seed, R., Bray, J.D., Stewart, J.P., Durgunoglu, H.T., Lettis, W., Tolga Yilmaz, M., 2004. Liquefaction-Induced lateral spreading at Izmit Bay during the Kocaeli (Izmit)-Turkey earthquake. J. Geotech. Geoenviron. 132.
Chaytor, J.D., Twichell, D.C., ten Brink, U.S., 2011. A reevaluation of the Munson-Nygren-Retriever submarine landslide complex, Georges Bank Lower Slope, Western North Atlantic. In: Yamada, Y.e.a. (Ed.), Submarine Mass Movements And Their Consequences, Volume 31. Springer, 17-21 June.
Clare, M.A., Vardy, M.E., Cartigny, M.J., Talling, P.J., Himsworth, M.D., Dix, J.K., Harris, J.M., Whitehouse, R.J., Belal, M., 2017. Direct monitoring of active geohazards: emerging geophysical tools for deep-water assessments. Near Surf. Geophys. 15 (4), 427–444.
Clare, M., Chaytor, J., Dabson, O., Gamboa, D., Georgiopoulou, A., Eady, A., Hunt, J., Jackson, C., Katz, O., Krastel, S., León, R., Micallef, A., Moernaut, J., Moriconi, R., Moscardelli, L., Mueller, C., Normandeau, A., Patacci, M., Steventon, M., Urlaub, M., Völker, D., Wood, L., Jobe, Z., 2018. A consistent global approach for the morphometric characterization of subaqueous landslides. In: Lintern, D.G., Mosher, D.C., Moscardelli, L.G., Bobrowsky, P.T., Campbell, C., Chaytor, J.D., Clague, J.J., Georgiopoulou, A., Lajeunesse, P., Normandeau, A., Piper, D.J.W., Scherwath, M., Stacey, C., Turmel, D. (Eds.), Subqueous Mass Movements, Volume 477. Geological Society, London.
Coleman, J.M., Prior, D.B., 1978. Submarine Landslides in the Mississippi River Delta, Offshore Technology Conference, Houston, Texas. May 8-11.
Collot, J.Y., Lewis, K.B., Lamarche, G., Lallemand, S., 2001. The giant Ruatoria debris avalanche on the northern Hikurangi margin,New Zealand: result of oblique seamount subduction. J. Geophys. Res. Solid Earth 106, 19271–19297.

Conti, S., Tosatti, G., 1993. Landslides affecting tabular rocks in complex geological situations: the case of Sasso di Simone and Simoncello (northern Apennines, Italy). In: Proceedings Landslides. Proceedings of Seventh ICFL, Czech and Slovak Republics Balkema, Rotterdam, pp. 219–224, 28 August–15 September.
Cruden, D.M., Varnes, D.J., 1996. Landslide types and processes. In: Turner, A.K., Schuster, R.L. (Eds.), Landslides Investigation And Mitigation, Volume 247. Transportation research board, US, National Research Council, Washington, DC, pp. 36–75.
Crutchley, G.J., Elger, J., Kuhlmann, J., Mountjoy, J.J., Orpin, A., Georgiopoulou, A., Carey, J., Dugan, B., Cardona, S., Han, S., Cook, A., Screaton, E.J., Pecher, I.A., Barnes, P., Huhn, K., 2022. Investigating the basal shear zone of the Submarine Tuaheni Landslide Complex, New Zealand: a core-log-seismic integration study. J. Geophys. Res. Solid Earth 127 p. e2021JB021997.
Cubrinovski, M., Robinson, K., 2016. Lateral spreading: evidence and interpretation from the 2010–2011 Christchurch earthquakes. Soil Dyn. Earthq. Eng. 91, 187–201.
Cubrinovski, M., Green, R.A.E., Allen, J., Ashford, S., Bowman, E., Bradley, B., Cox, B., Cubrinowski, M., Green, R., Hutchinson, T., Kavazanijan, E., Orense, R., Pender, M., Quigley, M., Wotherspoon, L., 2010. In: Geotechnical Reconnaissance of the 2010 Darfield (Canterbury) Earthquake Bulletin of the New Zealand Society for Earthquake Engineering, vol. 43, pp. 243–320 no. 4.
De Pascale, G.P., Bachhuber, J.L., Rathje, E., Hu, J., Almond, P., Ruegg, C., Finnemore, M., 2016. Geology of liquefaction-induced lateral spreading, new results from Christchurch, New Zealand. In: Proceedings SCEC (Southern California Earthquake Center) Annual Meeting.
Demers, D., Robitaille, D., Locat, P., Potvin, J., 2014. Inventory of large landslides in sensitive clay in the Province of Quebec, Canada: preliminary analysis. In: L'Heureux, J.-S. (Ed.), Landslides in Sensitive Clays: From Geosciences to Risk Management, Volume 36.
Demers, D., Robitaille, D., Lavoie, A., Paradis, S., Fortin, A., Ouellet, D., 2017. The use of Lidar airborne data for retrogressive landslides inventory in sensitive clays, Quebec, Canada. In: Thakur, V., L'Heureux, J.-S., Locat, A. (Eds.), Landslides in Sensitive Clays: From Research to Implementation. Springer, Netherlands, pp. 279–288.
Dey, R., Hawlader, B.C., Phillips, R., Soga, K., 2015. Large deformation finite element modelling of progressive failure leading to spread in sensitive clay slopes. Geotechnique 65 (8), 657–668.
Dey, R., Hawlader, B.C., Phillips, R., Soga, K., 2016. Numerical modelling of submarine landslides with sensitive clay layers. Géotechnique 66 (6), 454–468.
Durante, M.G., Rathje, E.M., 2021. An exploration of the use of machine learning to predict lateral spreading. Earthq.Spectra 37 (4), 2288–2314.
Evans, D., Harrison, Z., Shannon, P.M., Laberg, J.S., Nielsend, T., Ayers, T., Holmesa, R., Hoult, R.J., Lindberg, B., Haflidason, H., Long, D., Kuijpers, A., Andersen, E.S., Bryn, P., 2005. Palaeoslides and other mass failures of Pliocene to Pleistocene age along the Atlantic continental margin of NW Europe. Mar. Pet. Geol. 22, 1131–1148.
Field, M.E., Gardner, J.V., Jennings, A.E., Edwards, B.D., 1982. Earthquake-induced sediment failures on a 0.25° slope, Klamath River delta, California. Geology 10.
Gadd, N.R., 1975. Geology of Leda clay. M.Sc Thesis. In: Proceedings 4th Guelph Symposium on Geomorphology, Volume Mass Wasting. Geo Abstracts Ltd., pp. 137–151, 147 pp.
Gatter, R., Clare, M.A., Hunt, J.E., Watts, M., Madhusudhan, B.N., Talling, P.J., Huhn, K., 2020. A multi-disciplinary investigation of the AFEN Slide: the relationship between contourites and submarine landslides. In: Georgiopoulou, A., Amy, L.A., Benetti, S., Chaytor, J.D., Clare, M.A., Gamboa, D., Haughton, P.D.W., Moernaut, J., Mountjoy, J.J. (Eds.), Subaqueous Mass Movements And Their Consequences: Advances in Process Understanding, Monitoring And Hazard Assessments, Volume Special Publications. Geological Society, London.
Geertsema, M., 2004. A Composite Earthflow-spread in Sensitive Glaciomarine Sediments Near Terrace, British Columbia. M.Sc Thesis. University of Alberta, 147 pp.
Geertsema, M., Torrance, J.K., 2005. Quick clay from the Mink Creek landslide near terrace British Columbia: geotechnical properties, mineralogy and geochemistry. Can. Geotech. J. 42, 907–918.
Giona Bucci, M., Tuttle, M.P., 2021. Liquefaction susceptibility and hazard mapping: insights from case histories of earthquake-induced liquefaction. In: Owen, L. (Ed.), Treatise on Geomorphology, Second edition.
Glen, 2021. Spearman Rank Correlation (Spearman's Rho): Definition And How to Calculate It, Volume 2021. from StatisticsHowTo.com.
Greene, H.G., Murai, L.Y., Watts, P., Maher, N.A., Fisher, M.A., Paull, C.E., Eichhubl, P., 2006. Submarine landslides in the Santa Barbara Channel as potential tsunami sources. Nat. Hazard Earth Syst. Sci. 6, 63–88.
Gregersen, O., 1981. The quick clay landslide in Rissa, Norway. In: Proceedings 10th International Conference on Soil Mechanics And Foundation Engineering Stockholm, Volume 3, pp. 421–426.
Gregersen, O., Loken, T., 1974. 1979, the quick-clay slide at Baastad, Norway. Eng. Geol. 14 (2–3), 183–196.
Grondin, G., Demers, D., 1996. The 1989 Saint Liguori flakeslide: characterization and remedial works. In: Proceedings 7th International Symposium on Landslides, Trondheim, Norway, pp. 743–748, 17-21 June.
Haflidason, H., Sejrup, H.P., Nygard, A., Mienert, J., Bryn, P., Lien, R., Forsberg, C.F., Berg, K., Masson, D.G., 2004. The Storegga slide: architecture, geometry and slide development. Mar. Geol. 213 (1–4), 201–234.
Hjelstuen, B.O., Grinde, S., 2015. 3D seismic investigations of Pleistocene mass transport deposits and glacigenic debris flows on the North Sea Fan, NE Atlantic margin. In: Lamarche, G. (Ed.), Submarine Mass Movements And Their Consequences, Vol. 41. Springer International Publishing, Switzerland.
Hogan, K.A., Vanneste, M., Dowdeswell, J.A., Mienert, J., 2016. Geomorphology of the huge Hinlopen-Yermak landslide on the northern Svalbard margin. <sb: contribution><sb:title>Geol. Soc.</sb:title></sb:contribution><sb:host><sb: issue><sb:series><sb:title>Lond. Mem.</sb:title></sb:series></sb:issue></sb: host> 46, 415–416.
Holzer, T.L.c., 1998. The Loma Prieta, California, Earthquake of October 17, 1989-Liquefaction. United States Geological Survey.
Hughes Clarke, J.E., Vidiera Marques, C.R., Pratomo, D., 2014. Imaging active mass-wasting and sediment flows on a Fjord Delta, Squamish, British Columbia. In: Krastel, S. (Ed.), Submarine Mass Movements And Their Consequences, Volume 37. Springer International Publishing, Switzerland, pp. 249–260.
Huhnerbach, V., Masson, D.G., 2004. Landslides in the North Atlantic and its adjacent seas: an analysis of their morphology, setting and behaviour. Mar. Geol. 213, 343–362.
Hungr, O., Leroueil, S., Picarelli, S., 2014. The Varnes classification of landslide types, an update. Landslides 11, 167–194.
Hutchinson, D.J., 1965. In: The Landslide of February 1959 at Vibstad in Namdalen. Norwegian Geotechnical Institute, Oslo, Norway, pp. 1–16.
Ishihara, K., 1985. Stability of natural soil deposits during earthquakes. In: Proceedings Eleventh International Conference on Soil Mechanics And Foundation Engineering, San Francisco, Volume 1, pp. 321–376.
Kawakami, F., Asada, A., 1966. Damage to the ground and earth structures by the Niigata earthquake of June 16, 1964. In: Soils And Foundations, vol. 6. Japanese Society of Soil Mechanics and Foundation Engineering, pp. 14–30 no. 1.
Kerr, P.F., Milling Drew, I., 1968. Quick clay slides in the U.S.A. Eng. Geol. 2 (4), 215–238.
Kramer, S.L., Seed, H.B., 1988. Initiation of soil liquefaction under static loading conditions. J. Geotech. Eng. 114 (4), 412–430.
Krastel, S., Schmincke, H.-U.L., Jacobs, C., Rihm, R., Le Bas, R.P., Alibis, B., 2001. Submarine landslides around the Canary Islands. J.Geophys.Res. 106 (B3), 3977–3997.
Kvalstad, T.J., Andersen, L., Forsberg, C.F., Berg, K., Bryn, P., Wangen, M., 2005. The Storegga slide: evaluation of triggering sources and slide mechanics. Mar. Pet. Geol. 22, 245–256.
La Rochelle, P., Chagnon, J.Y., Lefebvre, G., 1970. Regional geology and landslides in the marine clay deposits of eastern Canada. Can. Geotech. J. 7, 145–156.
Laberg, J.S., Camerlenghi, A., 2008. The significance of contourites for submarine slope stability. In: van Loon, A.J., Rebesco, M., Camerlenghi, A. (Eds.), Contourites, Volume 60. Elsevier, Amsterdam, The Netherlands.
Laberg, J.S., Vorren, T.O., 2000. The Traenadjupet Slide, offshore Norway morphology, evacuation and triggering mechanism. Mar. Geol. 171, 95–114.
Laberg, J.S., Dahlgren, T., Vorren, T.O., Haflidason, H., Bryn, P., 2001. Seismic analysis of Cenozoic contourite drift development in the Northern Norwegian Sea. Mar. Geophys. Res. 22, 401–416.
Laberg, J.S., Vorren, T.O., Mienert, J.D.E., Lindberg, B., Ottesen, D., Kenyon, N.H., Henriksen, S., 2002. Late Quaternary palaeoenvironment and chronology in the Traenadjupet Slide area offshore Norway. Mar.Geol. 188, 35–60.
Lastras, G., Canals, M., Urgeles, R., 2003. Lessons from sea-floor and subsea-floor imagery of the Big'95 debris flow scar and deposit. In: Locart, J., Mienert, J. (Eds.), Submarine Mass Movements And Their Consequences. Kluwer Academic Publishers, Dordrecht, pp. 425–431.
Lastras, G., Canals, M., Amblas, D., Ivanov, M., Dennielou, B., Droz, L., Akhmetzhanov, A., 2006. Eivissa slides, western Mediterranean Sea: morphology and processes. Geo-Mar. Lett. 26, 225–233.
Lefebvre, G., 1996. Soft sensitive clays. In: Science, N.A. o. (Ed.), Landslides: Investigation And Mitigation, Volume Special Report 247. Turner, A. K. Schuster, R. L, Washington, p. 685.
Li, W., Alves, T.M., Urlaub, M., Georgiopoulou, A.I.K., Wynn, R.B.F.G., Meyer, M., Repschläger, J., Berndt, C., Krastel, S., 2016. Morphology, age and sediment dynamics of the upper headwall of the Sahara Slide Complex, Northwest Africa: evidence for a large Late Holocene failure. Mar.Geol. 393, 109–123.
Lindberg, B., Laberg, J.S., Vorren, T.O., 2004. The Nyk Slide-morphology, progression and age of a partly buried submarine slide offshore mid-Norway. Mar. Geol. 213, 277–289.
Lingwall, B.N., Gillins, D., Bunn, M.D., 2018. An update to the great earthquake lateral spread case history database. In: IFCEE 2018: Recent Developments in Geotechnical Engineering Practice, Orlando, Florida.
Liu, Z., L'Heureux, J.-S., Glimsdal, S., Lacasse, S., 2021. Modelling of mobility of Rissa landslide and following tsunami. Comput. Geotech. 140, 104388.
Locat, J., Lee, H.J., 2002. Submarine landslides: advances and challenges. Can. Geotech. J. 39, 193–212.
Locat, J., Leroueil, S., Locat, A., Lee, H., 2014. Weak layers: their definition and classification from a geotechnical perspective. In: Krastel, S., Behrmann, J.H., Volker, D., Stipp, M., Berndt, C., Urgeles, R., Chaytor, J., Huhn, K., Strasser, M., Harbitz, C.B. (Eds.), Submarine Mass Movements And Their Consequences, Advances in Natural And Technological Hazards Research, Volume 37. Springer International Publishing, Switzerland, Cham, pp. 3–12.
Locat, P., Demers, D., Locat, A., Leroueil, S., 2015. Investigations complementaires du glissement de terrain de Lemieux de 1993 sur la rivièreNation Sud A lemieux, Ontario. In: Proceedings 68th Canadian Geotechnical Conference, GEOQuebec 2015, Quebec City, 20-23 September 2015.
Locat, A., Locat, P., Demers, D., Leroueil, S., Robitaille, D., Lefebvre, G., 2017. The Saint-Jude landslide of 10 May 2010, Quebec, Canada: investigation and characterization of the landslideand its failure mechanism. Can. Geotech. J. 54 (10), 1357–1374.
van Loon, A.J.T., Pisarska-Jamrozy, M., Nartiss, M., Krievans, M., Soms, J., 2016. Seismites resulting from high-frequency, high-magnitude earthquakes in Latvia caused by Late Glacial glacio-isostatic uplift. J. Palaeogeogr. 5 (4), 363–380.

Lowe, D., Moon, V.G., Mills, P., Kluger, M., Churchman, G., de Lange, W., Hepp, D., Kreiter, S., Morz, T., 2017. Sensitive pyroclastic soils in the Bay of Plenty, New Zealand: microstructure to failure mechanisms. In: 20th Symposium of the New Zealand Geotechnical Society, Napier.
Magri, O., Mantovani, M., Pasuto, A., Soldati, M., 2008. Geomorphological investigation and monitoring of lateral spreading along the north-west coast of Malta. Geogr. Fis. Din. Quat. 31 (2), 171–180.
Masson, D.G., Harbitz, C.B., Wynn, R.B., PEdersen, G., Lohvholt, F., 2006. Submarine landslides-Processes, triggers and hazard prediction. Philos.Trans.R.Soc. 364, 2009–2039.
McCulloch, D.S., Bonilla, M.G., 1970. Effects of the Earthquake of March 27, 1964, on the Alaska Railroad, 161.
Micallef, A., Masson, D.G., Berndt, C., Dorrik, A., Stow, V., 2007. Morphology and mechanics of submarine spreading: a case study from the Storegga slide. J. Geophys. Res. 112, F03023.
Micallef, A., Masson, D.G., Berndt, C., Stow, D.A.V., 2009. Development and mass movement processes of the north eastern Storegga Slide. Quat. Sci. Rev. v. 28, 433–448.
Micallef, A., Georgiopoulou, A., Mountjoy, J., Huvennee, V.A.I., Lo Iaconoe, C., Le Base, T., Del Carlo, P., Cunaroo Oteroa, D., 2016. Outer shelf seafloor geomorphology along a carbonate escarpment: the eastern Malta Plateau, Mediterranean Sea. Cont. Shelf Res. 131, 12–27.
Miramontes, E., Garziglia, S., Sultan, N., Jouet, G., Cattaneo, A., 2018. Morphological control of slope instability in contourites: a geotechnical approach. Landslides 15, 1085–1095.
Mollard, J.D., Hughes, G.T., 1973. Earthflows in the Grondines and the Trois Rivieres Areas, Quebec: discussion. Can. J. Earth Sci. 10 (2), 324–326.
Moon, V.G., Cunningham, M.J., Wyatt, J., Lowe, D.J., 2013. Landslides in sensitive soils, Tauranga, New Zealand. In: Proceedings NZGS Geotechnical Symposium, Queenstown, 38, pp. 537–544.
Morsilli, M., Moretti, M., 2011. Gli slumps del Gargano: paleofrane sottomarine del Cretaceo Inferiore. Geoitalia 36, 47–50.
Mountjoy, J.J., McKean, J., Barnes, P.M., Pettinga, J.R., 2009. Terrestrial-style slow-moving earthflow kinematics in a submarine landslide complex. Mar. Geol. 267, 114–127.
Mountjoy, J.J., Xiaoming, W., Susi, W., Fitzsimons, S., Howarth, J., Orpin, A.R., Power, W., 2018. Tsunami hazard from lacustrine mass wasting in Lake Tekapo, New Zealand. In: Lintern, D.G., Mosher, D.C., Moscardelli, L.G., Bobrowski, P.T., Campbell, C., Chaytor, J.D., Clague, J.J., Georgiopolou, A., Lajeunesse, P., Normandeau, A., Piper, D.J.W., Scherwath, M., Stacey, C., Turmel, D. (Eds.), Subaqueous Mass Movements, Volume 477. Geological Society, London.
Mulder, T., Cochonat, P., 1996. Classification of offshore mass movements. J. Sediment. Res. 66 (1), 43–57.
National Research Council, 1985. Liquefaction of Soils During Earthquakes. National Academy Press, Washington D.C.
Normandeau, S., Campbell, C., Piper, D.J., Jenner, K., 2018. New evidence for a major late Quaternary submarine landslide on the external western levee of Laurentian Fan. In: Lintern, D.G., Mosher, D.C., Moscardelli, L.G., Bobrowsky, P.T., Campbell, C., Chaytor, J.D., Clague, J.J., Georgiopoulou, A., Lajeunesse, P., Normandeau, A., Piper, D.J.W., Scherwath, M., Stacey, C., Turmel, D. (Eds.), Subaqueous Mass Movements, Volume 477. Geological Society.
Nouguès, A., Sultan, N., Cattaneo, A., Dan, G., Yelles, K., team, P., 2009. Detailed analysis of a submarine landslide (SAR-27) in the deep basin offshore Algiers (Western Mediterranean). In: al., D.C.M. e (Ed.), Submarine Mass Movements And Their Consequences, Volume 28. Springer Science.
Ogata, K., Mountjoy, J.J., Pini, G.A., Festa, A., Tinterri, R., 2014. Shear zone liquefaction in mass transport deposit emplacement: a multi-scale integration of seismic reflection and outcrop data. Mar. Geol. 356, 50–64.
Olson, S.M., Johnson, C.I., 2008. Analyzing liquefaction-induced lateral spreads using strength ratios. J. Geotech. Geoenviron. 134, 1035–1049.
Pasuto, A., Soldati, M., 2013. Lateral spreading. In: Shroder, J., Marston, R.A., Stoffel, M. (Eds.), Treatise on Geomorphology, Volume 7. Academic Press, San Diego,CA, pp. 239–248.
Pasuto, A., Soldati, M., Tecca, P.R., 2022. Lateral spread: from rock to soil spreading. In: Shroder, J.F. (Ed.), Treatise on Geomorphology, , Second ed.Volume 5. Academic Press, Cambridge Massachusetts, pp. 169–182.
Paull, C.K., Dallimore, S.R., Caress, D.W., Gwiazda, R., Lundsten, E., Anderson, K., Melling, H., Jin, Y.K., Duchesne, M.J., Kang, S.-G., Kim, S., Riedel, M., King, E.L., Lorenson, T., 2021. A 100-km wide slump along the upper slope of the Canadian Arctic was likely preconditioned for failure by brackish pore water flushing. Mar. Geol. 435, 106453.
Perret, D., Therrien, J., Locat, P., Demers, D., 2019. Influence of surficial crusts on the development of spreads and flows in Eastern Canadian sensitive clays. In: GeoSt. John's 2019.
Piper, J.W.D., 2005. Late Cenozoic evolution of the continental margin of eastern Canada. Nor. J. Geol. 85, 305–318.
Piper, D.J.W., Cochonat, P., Morrison, M.L., 1999. The sequence of events around the epicentre of the 1929 Grand Banks earthquake: initiation of debris flow and turbidity current inferred from sidescan sonar. Sedimentology 46, 79–97.
Pisarska-Jamroży, M., Woźniak, P., 2019. Debris flow and glacioisostatic-induced soft-sediment deformation structures in a Pleistocene glaciolacustrine fan: the southern Baltic Sea coast, Poland. Geomorphology 326, 225–238.
Prampolini, M., Foglini, F., Micallef, A., Soldati, M., Taviani, M., 2019. Malta's submerged landscapes and landforms. In: Gauci, R., Schembri, J. (Eds.), Landscapes And Landforms of the Maltese Island, Volume World Geomorphological Landscapes. Springer, Cham.
Prior, D.B., Coleman, J.M., 1978. Disintegrating retrogressive landslides on very-low-angle subaqueous slopes,Mississippi Delta. Mar. Geotechnol. 3 (1), 37–60.
Prior, D.B., Bornhold, B.D., Coleman, J.M., Bryant, W.R., 1982. Morphology of a submarine slide, Kitimat Arm, British Columbia. Geology 10, 588–592.
Puzrin, A.M., Germanovich, L.N., 2005. The growth of shear bands in the catastrophic failure of soils. Proc. R. Soc. Lond. Ser. A 461 (2056), 1199–1228.
Puzrin, A.M., Gray, T.E., Hill, A.J., 2015. Significance of the actual nonlinear slope geometry for catastrophic failure in submarine landslides. Proc. R. Soc. Acad. 471, 20140772.
Quinn, P.E., Hutchinson, D.J., Diederichs, M.S., Rowe, R.K., 2011. Characteristics of large landslides in sensitive clay in relation to susceptibility, hazard and risk. Can. Geotech. J. 48, 1212–1232.
Quinn, P.E., Diederichs, M.S., Rowe, R.K., Hutchinson, D.J., 2012. Development of progressive failure in sensitive clay slopes. Can. Geotech. J. 49 (7), 782–795.
Rebesco, M., Hernandez-Molina, F.J.D.V.R., Wahlin, A., 2014. Contourites and associated sediments controlled by deep-water circulation processes: state-of-the-art and future considerations. Mar.Geol. 352, 111–154.
Rees, D., 2000. Essential Statistics. Chapman and Hall/CRC, Lindsey, J., Zidek, J., and Chatfield, C.
Sammartini, M., Camerlenghi, A., Budillon, F., Insinga, D.D., Zgur, F., Conforti, A., Iorio, M., Romeo, R., Tonielli, R., 2018. Open-slope, translational submarine landslide in a tectonically active volcanic continental margin Q1 (Licosa submarine landslide, southern Tyrrhenian Sea). In: Lintern, D.G., Mosher, D.C., Moscardelli, L. G., Bobrowsky, P.T., Campbell, C., Chaytor, J.D., Clague, J.J., Georgiopoulou, A., Lajeunesse, P., Normandeau, A., Piper, D.J.W., Scherwath, M., Stacey, C., Turmel, D. (Eds.), Subaqueous Mass Movements, Volume 477. Geological Society, London.
Savini, A., Krastel, S., Micallef, A., 2022. Perspectives on submarine geomorphology: an introduction. In: Treatise on Geomorphology, , Second ed.Volume 8, pp. 811–829.
Schnellmann, M., Anselmetti, F.S., Giardini, D., McKenzie, J.A., 2005. Mass movement induced fold-and-thurst belt structures in unconsolidated sediments in Lake Lucerne (Switzerland). Sedimentology 52 (2), 271–289.
Schwab, J.W., Geertsema, M., Blais-Stevens, A., 2004. The Khyex River landslide of November 20, 2003, Prince Rupert British Columbia, Canada. Landslides 1, 243–246.
Scott, R.F., Zuekerman, K.A., 1973. Sand blows and liquefaction. In: The Great Alaska Earthquake of 1964. National Academy of Sciences, pp. 179–189.
Seed, H.B., Tokimatsu, K., Harder, L.F., Chung, R.M., 1985. The influence of SPT procedures in soil liquefaction resistance evaluations. J.Geotech.Eng.ASCE 111 (12), 1425–1445.
Seed, H.B., Seed, R.B., Schlosser, F., Blondeau, F., Juran, I., 1988. The Landslide at the Port of Nice on October 16, 1979. Earthquake Engineering Research Centre, University of California at Berkeley.
Solberg, I.L., Hansen, L., Rokoengen, K., 2007. Distribution of clay slides in fjord-valley deposits and their role in valley development, example from mid-Norway. In: Proceedings 1st North American Landslide Conference, Vail, Colo, Denver, Colorado, 3-10 June 2007, Volume 23. AEG Special Publication, pp. 472–487.
Solberg, I.-L., Nordhal, B., Hansen, L., Ove Grotan, B., Gulbrandsen, G., 2017. The Norwegian National Database for Ground Investigations (NADAG): a tool to assist in landslide hazard zonation and other quick-clay related issues. In: Thakur, V., L'Heureux, J.S., Locat, A. (Eds.), Landslides in Sensitive Clays: From Research to Implementation, Volume 46. Springer, Switzerland.
Soldati, M., Barrows, T.T., Prampolini, M., Fifield, K.L., 2018. Cosmogenic exposure dating constraints for coastal landslide evolution on the Island of Malta (Mediterranean Sea). J. Coast. Conserv. 22, 831–844.
Spalluto, L., Moretti, M., Festa, V., Tropeano, M., 2007. Seismically-induced slumps in Lower-Maastrichtian peritidal carbonates of the Apulian Platform (southern Italy). Sediment. Geol. 196, 81–98.
Steffen, H., Olesen, O., Sutinen, R., 2021. Glacially-triggered Faulting. Cambridge University Press, Cambridge. Steffen, H., Olesen, O., and Sutinen, R.
Stoecklin, A., Friedli, B., Puzrin, A.M., 2017. Sedimentation as a control for large submarine landslides: mechanical modeling and analysis of the Santa Barbara Basin. <sb:contribution><sb:title>J. Geophys. Res. Solid</sb:title></sb:contribution><sb:host><sb:issue><sb:series><sb:title>Earth</sb:title></sb:series></sb:issue></sb:host> 112, 8645–8663.
Strachan, L.J., 2004. Slump-initiated and controlled syndepositional sandstone remobilization: an example from the Namurian of Couty Clare, Ireland. Sedimentology 49 (1), 25–41.
Strachan, L.J., Alsop, G.I., 2006. Slump folds as estimators of palaeoslope: a case study from the Fisherstreet Slump of County Clare, Ireland. Basin Res. 18 (4), 451–470.
Taboada-Urtuzuastegui, V., Dobry, R., 1998. Centrifuge modeling of earthquake-induced lateral spreading in sand. J. Geotech. Geoenviron. Eng. 124 (12), 1195–1206.
Talling, P., Clare, M., Urlaub, M., Pope, E., Hunt, J., Watt, S., 2014. Large submarine landslides on continental slopes: geohazards,methane release, and climate change. Oceanography 27 (2), 32–45.
Terzaghi, K., Peck, R.B., Mesri, G., 1996. Soil Mechanics in Engineering Practice, Wiley-Interscience publication. John Wiley & Sons, Canada.
Thakur, V., L'Heureux, J.-S., A, L., 2017. Landslides in sensitive clays, from research to implementation. In: Advances in Natural And Technological Hazards Research. Springer, Switzerland. Thakur, V., L'Heureux, J.-S., and A., L.
Tinsley, J.C., Egan, J.A., Kayen, R.E., Bennet, M.J., Kropp, A., Holzer, T.L., 1998. Appendix: maps and descriptions of liquefaction and associated effects. In: Holzer, T. L. (Ed.), quake of October 17 1989–Liquefaction, U.S. Geological Survey Professional Paper, Volume 1551-B, pp. B287–B314.
Tremblay-Auger, F., Locat, A., Leroueil, S., Locat, P., Demers, D., Therrien, J., Mompin, R., 2020. The 2016 landslide at Saint Luc de Vincennes, Quebec:

geotechnical and morphological analysis of a combined flowslide and spread. Can. Geotech.J. 58, 295–304.
Tuttle, M., Barstow, N., 1996. Liquefaction-related ground failure: a case study in the New Madrid Seismic Zone,Central United States. Bull. Seismol. Soc. Am. 86 (3), 636–645.
Updike, R.G., Egan, J.A., Moriwaki, Y., Idriss, L.M., Moses, T.L., 1988. A model for earthquake-induced translatory landslides in Quaternary sediments. Geol. Soc. Am. Bull. 100, 783–792.
Urgeles, R., Camerlenghi, A., 2013. Submarine landslides of the Mediterranean Sea: trigger mechanisms, dynamics, and frequency-magnitude distribution. J. Geophys. Res. 118, 2600–2618.
Vanneste, M., Mienert, J., Bunz, S., 2006. The Hinlopen Slide: a giant submarine slope failure on the northern Svalbard margin,Artic Ocean. Earth Planet. Sci. Lett. 245, 373–388.
Varnes, D.J., 1978. Slope movement types and processes. In: Shuster, R.L., Krizek, R.J. (Eds.), Landslides Analysis And Control, Volume Special Report 176. National Research Council, Washington, pp. 11–33.
Wallace, R.H., 1965. Effects of the Earthquake of March 27,1964, at Anchorage, Alaska-effects on communities: United States Department of the Interior, Professional Paper 542. USGS. https://doi.org/10.3133/pp542.
Wang, C., 2020. Numerical Study of Large Deformation Retrogressive Landslides in Sensitive Clay Triggered by Toe Erosion And Earthquake [PhD Memorial University of Newfoundland.
Wang, C., Hawlader, B., Perret, D., Soga, K., 2020. Effects of geometry and soil properties on type and retrogression of landslides in sensitive clays. Can. Geotech. J. 1–15.
Wang, C., Hawlader, B., Perret, D., Soga, K., Chen, J., 2021. Modeling of initial stresses and seepage for large deformation finite-element simulation of sensitive clay landslides. J. Geotech. Geoenviron. Eng. 147 (11), 04021111.
Wilson, C.K., Long, D., Bulat, J., 2004. The morphology, setting and processes of the Afen Slide. Mar. Geol. 213, 149–167.
Wu, N.A.-L., Jackson, C.D., Johnson, H.M., Hodgson, D., Clare, M.A., Nugraha, H.A., Li, W., 2021. The formation and implications of giant blocks and fluid escape structures in submarine lateral spreads. Basin Res. 00, 1–20.
Youd, T.L., 1978. Major cause of earthquake damage is ground failure. In: Civil Engineering, Environmental Design/Civil Engineered. ASCE, pp. 47–51 [PhD Memorial University of Newfoundland.
Youd, T.L., 1995. Liquefaction-induced lateral ground displacement. In: Third International Conference on Recent Advances in Geotechnical Earthquake Engineering And Soil Dynamics April 2-7, St. Louis, Missouri.